TU Delft

Delft University of Technology

Assessing the Role of Pt Clusters on TiO_2 (P25) on the Photocatalytic Degradation of Acid Blue 9 and Rhodamine B

Benz, Dominik; Felter, Kevin M.; Köser, Jan; Thöming, Jorg; Mul, Guido; Grozema, Ferdinand C.; Hintzen, Hubertus T.; Kreutzer, Michiel T.; Van Ommen, J. Ruud

DOI
10.1021/acs.jpcc.0c00926

Publication date
2020

Document Version
Final published version

Published in
Journal of Physical Chemistry C

Citation (APA)
Benz, D., Felter, K. M., Köser, J., Thöming, J., Mul, G., Grozema, F. C., Hintzen, H. T., Kreutzer, M. T., & Van Ommen, J. R. (2020). Assessing the Role of Pt Clusters on TiO_2 (P25) on the Photocatalytic Degradation of Acid Blue 9 and Rhodamine B. *Journal of Physical Chemistry C*, *124*(15), 8269-8278. https://doi.org/10.1021/acs.jpcc.0c00926

Important note
To cite this publication, please use the final published version (if applicable).
Please check the document version above.

Copyright
Other than for strictly personal use, it is not permitted to download, forward or distribute the text or part of it, without the consent of the author(s) and/or copyright holder(s), unless the work is under an open content license such as Creative Commons.

Takedown policy
Please contact us and provide details if you believe this document breaches copyrights.
We will remove access to the work immediately and investigate your claim.

This work is downloaded from Delft University of Technology.
For technical reasons the number of authors shown on this cover page is limited to a maximum of 10.

This is an open access article published under a Creative Commons Non-Commercial No Derivative Works (CC-BY-NC-ND) Attribution License, which permits copying and redistribution of the article, and creation of adaptations, all for non-commercial purposes.

ACS AUTHORCHOICE

THE JOURNAL OF PHYSICAL CHEMISTRY C

pubs.acs.org/JPCC

Article

Assessing the Role of Pt Clusters on TiO_2 (P25) on the Photocatalytic Degradation of Acid Blue 9 and Rhodamine B

Dominik Benz,* Kevin M. Felter, Jan Köser, Jorg Thöming, Guido Mul, Ferdinand C. Grozema, Hubertus T. Hintzen, Michiel T. Kreutzer, and J. Ruud van Ommen*

Cite This: J. Phys. Chem. C 2020, 124, 8269–8278

Read Online

ACCESS | Metrics & More | Article Recommendations | Supporting Information

ABSTRACT: The role of Pt on photocatalytic substrates such as TiO_2 (P25) for the decomposition of organic pollutants is still controversial in the scientific community. The well-observed behavior of an optimum catalytic activity as a function of the Pt loading is usually explained by the shift from charge separation to charge recombination behavior of Pt clusters. However, experiments supporting this explanation are still lacking to give a concise understanding of the effect of Pt on the photocatalytic activity. Here, we present an experimental study that tries to discriminate the different effects influencing the photocatalytic activity. Using atomic layer deposition in a fluidized bed reactor, we prepared TiO_2 (P25) samples with Pt loadings ranging from 0.04 wt % to around 3 wt %. In order to reveal the mechanism behind the photocatalytic behavior of Pt on P25, we investigated the different aspects (i.e., surface area, reactant adsorption, light absorption, charge transfer, and reaction pathway) of heterogeneous photocatalysis individually. In contrast to the often proposed prolonged lifetime of charge carriers in Pt-loaded TiO_2, we found that after collecting the excited electrons, Pt acts more as a recombination center independent of the amount of Pt deposited. Only when dissolved O_2 is present in the solution, charge recombination is suppressed by the subsequential consumption of electrons at the surface of the Pt clusters with the dissolved O_2 benefited by the improved O_2 adsorption on the Pt surface.

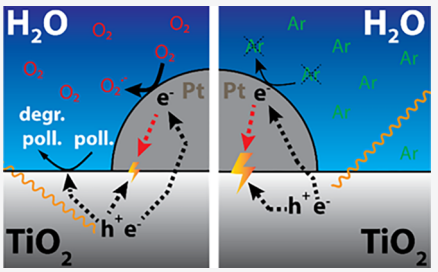

1. INTRODUCTION

Photocatalysis to clean water is a promising technology for tackling the rising problem of water pollution, especially in low-resource countries. Using materials such as TiO_2 and sunlight, many reports have shown the degradation of a range of pollutants in water.[1−6] However, the implementation in real-life remains challenging because of lack of efficiency. Getting insight into the working principles of the developed catalyst will especially help further developments such as combining materials in order to make even more active catalysts. In order to degrade organic pollutants using photocatalysis, generally four steps take place:[7,8]

(1) Adsorption of the reactants (pollutant, O_2, and H_2O) on the surface

(2) Light absorption and generation of charge carriers (e^-/h^+)

(3) Redox reaction on the surface creating hydroxyl radicals, superoxide radicals, or directly oxidizing the pollutant

(4) Desorption of products from the surface

Upon light excitation of the photocatalysts, an electron (e^-) is excited to the conduction band (CB), leaving a hole (h^+) in the valence band (VB). Those excited charges generate reactive oxygen species (ROS) such as superoxide radicals (O_2^{-}*) from e^-_{CB} and hydroxyl radicals (OH*) from h_{VB}^+. However, excited electrons are prone to recombine with holes, if not harvested efficiently, losing the potential for the preferred redox reaction to degrade organic pollutants.

According to this mechanism for the photocatalytic degradation of organic pollutants, three different events lead to the degradation of the pollutant:[4,9]

(1) The creation of superoxide radicals (O_2^{*-}) from the CB electrons and dissolved oxygen leads to the formation of OH* radicals which oxidize the pollutant subsequently to CO_2 and H_2O:

$$e_{CB}^- + O_2 \rightarrow O_2^{*-} \rightarrow \rightarrow OH$$
$$OH^* + \text{pollutant} \rightarrow \rightarrow \text{decomposed pollutant} \quad (1)$$

(2) The creation of OH* radicals from the reaction of H_2O or −OH groups at the surface with the VB holes which subsequently oxidize the pollutant:

$$H_2O + h_{VB}^+ \rightarrow OH^* + H^+ \quad (2)$$

Received: February 2, 2020
Revised: March 21, 2020
Published: March 24, 2020

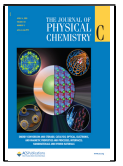

Downloaded via TU DELFT on May 25, 2020 at 16:06:19 (UTC).
See https://pubs.acs.org/sharingguidelines for options on how to legitimately share published articles.

© 2020 American Chemical Society

https://dx.doi.org/10.1021/acs.jpcc.0c00926
J. Phys. Chem. C 2020, 124, 8269−8278

$$-OH + h_{VB}^{+} \rightarrow OH^{*} \quad (3)$$

$$OH^{*} + \text{pollutant} \rightarrow \rightarrow \text{decomposed pollutant} \quad (4)$$

(3) Generated holes in the VB directly oxidize the pollutant:

$$\text{pollutant} + h_{VB}^{+} \rightarrow \text{pollutant}^{*+} \rightarrow \text{decomposed pollutant} \quad (5)$$

In order to improve the performance of a photocatalyst, several approaches are generally proposed: (i) enhance the affinity of the reactants toward the catalyst surface to improve proximity to ROS and therefore degradation probability; (ii) enhance the amount of light absorbed by the catalyst which results in more electron−hole pair generation; (iii) enhance the quantum yield by preventing charge recombination; or (iv) improving the desorption of the products from the surface.

Many publications claim to have found a better catalyst because of the improvement of one or more of those aspects, while a complete description of the materials' properties is generally lacking. Especially for photocatalysts, many properties influence the overall activity, which makes a complete analysis of the relationship to the final photocatalytic activity challenging. Apart from experimental design parameters such as catalyst concentration in the slurry, irradiation area, light intensity, and pollutant concentration, the materials' properties are the key to improve the intrinsic photocatalytic activity. Accessible reaction surface area, light absorption/bandgap, extrinsic quantum yield (how many separated charge carriers are created from the incident light that further react with the contaminant or generate ROS), and the affinity of the pollutants toward the surface play important roles and are related to the intrinsic material properties. In order to have insight into the difference in activity between various materials, all relevant properties should be taken into consideration and compared to enable the elaboration of the structure−activity relationships, which requires numerous characterization tools and analyses. For getting a complete picture of the prepared material, it is ubiquitous to address all these questions simultaneously.

The lack of an insight often leads to discussions on what is the real reason for enhancement or suppression in photocatalytic performance for the degradation of dyes as a function of the surface modification. Pt-decorated TiO_2 nanoparticles demonstrated in earlier studies an improved activity for dye degradation.[10−12] However, there exist still different theories why a low amount of platinum clusters onto P25 enhances the photocatalytic activity. The explanations include enhanced charge separation,[13−16] improved light absorption,[17] and better O_2 adsorption.[18−22] On the other hand, especially for higher Pt loadings, the photocatalytic activity drops as proposed in earlier research due to charge recombination.[18,23−25] However, this explanation seems contradictory because a change from charge separation to charge recombination purely based on Pt loading does not seem likely. With their purely theoretical approach, Muhich et al. provided a reasonable explanation stating that Pt serves as a recombination center independent of the loading, where electrons and holes recombine in the Pt cluster. On the other hand, they advocate the importance of dissolved O_2 in solution which adsorbs on the surface of Pt.[18] The objective of the current paper is to substantiate Muhich's et al. theoretical approach by an experimental study elaborating on the different effects Pt clusters can have on the surface of TiO_2 (P25) focused on the charge carrier kinetics and to investigate the importance of dissolved oxygen.

2. EXPERIMENTAL SECTION

2.1. Materials. TiO_2 nanoparticles [P25, mean diameter ≈ 21 nm, Brunauer−Emmett−Teller (BET) surface area of ∼54 $m^2\ g^{-1}$, information from supplier] were purchased from Evonik Industries (Hanau, Germany). Trimethyl-(methylcyclopentadienyl)platinum(IV) ($MeCpPtMe_3$) was obtained from Strem Chemicals and used as received. Acid Blue 9 (Brilliant Blue FCF) and rhodamine B were purchased from Sigma-Aldrich and were used without further purification.

2.2. Deposition. Prior to deposition, the TiO_2 powder was sieved with a 250 μm mesh to break and exclude larger agglomerates. Platinum was deposited on P25 using a homebuilt ALD setup in a fluidized bed under atmospheric pressure.[26,27] In brief, the powder was placed in a quartz glass column (diameter 26 mm, height 500 mm), which was then placed on a vertical vibration table (Paja 40/40-24) to assist fluidization. $(MeCp)PtMe_3$ was used as the Pt precursor, and oxygen gas was used as a counter reactant. For the ALD reactions, the Pt precursor was contained in a stainless-steel bubbler and heated to 70 °C, and the stainless steel lines, connecting both the Pt precursor and O_2 (grade 5.0) individually to the reactor, were heated to 90 °C to avoid precursor condensation. The glass reactor was heated to 100 °C throughout the experiment using an infrared lamp, which was placed parallel to the column, with feedback control. For every experiment, 1.5 g of P25 powder was placed in the reactor column. Nitrogen (grade 5.0), serving as a carrier gas for the precursor, was introduced through a distributor plate at the bottom of the column with a flow of 0.5 l/min resulting in a superficial gas velocity of 1.6 cm s^{-1} to ensure proper fluidization and distribution of the precursor. The deposition process consisted of sequential exposures of the powders to the Pt precursor (20 s to 5 min) and oxygen (5 min), separated by a purging step (5 min) using nitrogen as an inert gas.

After deposition, the powders were treated under an atmosphere of 5% H_2 in nitrogen (v/v) in a fixed bed reactor with a flow of 100 mL/min. The temperature was ramped up from room temperature to 200 °C with a rate of 2 °C/min and then was held constant for 5 min after which the powder was allowed to cool down to room temperature.

2.3. Characterization. For the inductively coupled plasma−optical emission spectrometry (ICP−OES) analysis, approximately 30 mg of sample was digested in 4.5 mL 30% HCl + 1.5 mL 65% HNO_3 + 0.2 mL 40% HF acid mixture using a microwave. The digestion duration in the microwave was 60 min. After the digestion, the samples were diluted to 50 mL with MQ water and analyzed with ICP−OES 5300DV. The samples were also diluted 20 times for Ti.

Transmission electron microscopy (TEM) pictures were acquired from a JEOL JEM1400 transmission electron microscope at 120 kV. As-deposited Pt:P25 nanoparticles were suspended in ethanol and transferred to Cu TEM grids (3.05 mm in diameter, Quantifoil).

X-ray photoelectron spectra (XPS) were recorded on a Thermo Fisher K-Alpha system using Al Kα radiation with a photon energy of 1486.7 eV. A sufficient amount of powders was immobilized on copper tape before loading into the XPS chamber. Scans were acquired using a 400 μm spot size, 55 eV pass energy, and 0.1 eV/step with charge neutralization. The peak positions were analyzed using the Thermo Avantage

https://dx.doi.org/10.1021/acs.jpcc.0c00926
J. Phys. Chem. C 2020, 124, 8269−8278

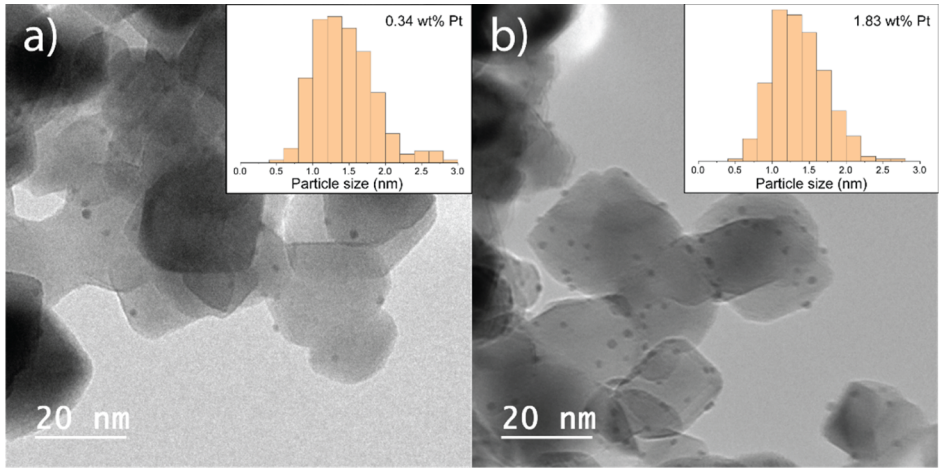

Figure 1. (a) TEM image of Pt clusters deposited on P25 (0.34 wt % Pt): the bigger particles represent the TiO_2 particles, and small black dots on the surface of TiO_2 indicate the Pt clusters. (b) TEM image of Pt clusters deposited on P25 (1.83. wt % Pt). Insets: particle size distribution of Pt clusters of corresponding samples.

software after SMART type background subtraction and calibrating the measurements by taking the C 1s peak as reference at 284.8 eV.

BET surface area was measured on a Micromeritics Tristar II 3020. The samples were degassed overnight at 150 °C to remove adsorbed water on the surface.

Measurements of the mean agglomerate diameter (*z*-average) in dispersion and the zeta-potential have been carried out at a Beckmann−Coulter DelsaNanoC (Krefeld, Germany). Prior to the measurement, 15 mg of powder in 15 mL (Milli-Q water) was dispersed by a sequence of 15 min stirring followed by sonication treatment for 20 s and an amplitude of 100% (200 W) using a Bandelin Sonopuls HD 3100 sonicator (Berlin, Germany). Afterward, the dispersion was stirred for another 15 min. The mean particle size (*z*-average diameter) was measured using the cumulant analysis by averaging ten measurements with the detector configuration at an angle of 165° respective to the incident light beam. Three independent samples were measured for each material. The zeta-potential measurements were executed using the correlating flow cell of the same instrument using the same dispersion protocol. The pH of the dispersions was measured after 5 min of submerging the pH electrode (Voltcraft pH-100ATC, Hirschau, Germany) into the freshly dispersed powder.

For adsorption measurements, the catalyst (2 g/L) was dispersed in a solution of Acid Blue 9 (16 mg/L_{aq}) or rhodamine B (12 mg/L_{aq}) under vigorous stirring. After distinct time intervals, a liquid sample was analyzed using UV/vis spectroscopy to measure the remaining concentration of the corresponding dye in solution.

UV/vis-DRS measurements were performed using a PerkinElmer-Lambda 900 spectrometer equipped with an integrating sphere device scanning from 200 to 800 nm. The reflectance for various samples was measured where Barium sulfate served as a reference for 100% reflection over the measured wavelength range.

The photoconductive behavior of the samples was measured with the time-resolved microwave conductivity technique (TRMC) on a custom-built setup described elsewhere.[28] The TRMC technique allows the measurement of the intrinsic photoconductivity of a sample without the need for external electrical contacts. A thin film sample was prepared on a quartz slide from a concentrated dispersion in ethanol by doctor blade coating and then dried at 80 °C for 30 min and placed in a microwave cavity cell. The sample was continuously exposed to continuous X-band microwaves at an approximate resonance frequency of 8.5 GHz that were generated by a Gunn diode. Photoexcitation of the sample occurred with 3.5 ns full width half maximum laser pulses of tunable wavelength (240−2200 nm) using an EKSPLA NT342B SH/SFG-10-AW Nd:YAG laser. Upon photoexcitation, free and mobile charge carriers were generated, that is, electrons and holes, that absorb part of the incident microwave power expressed as $\Delta P(t)/P$. The change in microwave power is proportional to a change in the photoconductance $\Delta G(t)$ as

$$\Delta P(t)/P = -K\Delta G(t)$$

Here K is a frequency-dependent sensitivity factor (40×10^3 S^{-1}) that follows from the resonance properties of the setup and the properties of the dielectric media present. The half-life of the transient photoconductance was used as a measure for charge transfer from TiO_2 to the Pt clusters on the hundred to microsecond timescale.

2.4. Photocatalytic Testing. Photocatalytic testing under saturated Ar and O_2 atmosphere was done in a 30 mL custom made quartz reactor with 15 mg of powder and a 30 mL solution of Acid Blue 9 (16 mg/L) or rhodamine B (12 mg/L) dissolved in deionized water under natural pH. For better dispersion and degassing, the powder was put into the solution of Acid Blue 9 or rhodamine B and sonicated in an ultrasonic bath (Ultrasonic Cleaner, USC−TH, VWR) for 10 min. For the experiments under an inert atmosphere, the solution was transferred into the reactor vessel in an N_2 glovebox to avoid exposure to the oxygen in the air. Afterward, the dispersion was stirred for 30 min under bubbling of Ar or O_2 gas in order to reach the desired atmosphere—inert versus saturated solution of dissolved O_2. The samples were irradiated using a 500 W deep UV mercury lamp (Ushio) and after distinct times samples of 0.5 mL were taken, filtered through a 0.45 μm PTFE filter, and the filtrate was then analyzed using a UV/vis spectrometer (Hach-Lange, DR5000, Düsseldorf, Germany) in a quartz glass cuvette with a thickness of 1 cm. A blank spectrum of water as the reaction medium was measured as a reference and automatically subtracted. The absorption was

https://dx.doi.org/10.1021/acs.jpcc.0c00926
J. Phys. Chem. C 2020, 124, 8269−8278

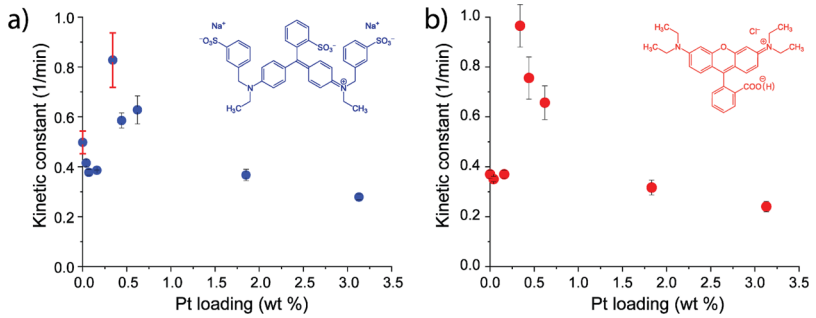

Figure 2. Kinetic constants for the degradation of (a) Acid Blue 9 and (b) rhodamine B: red error bars represent the standard error of repeated experiments, and black error bars indicate the standard error form the linear regression fitting the kinetic constant.

Table 1. Overview of the Main (Photo-)Catalytic Parameters as Related to Various Material Properties and Factors Influenced by Them and the Corresponding Analysis Tools

	material property	affects	analysis tool
general catalytic parameter	surface area	number of reaction sites	BET
	accessible surface area in solution/agglomeration of catalyst particles	diffusion/mass transfer	DLS
	surface charge	reactant adsorption	1) zeta-potential 2) amount of adsorbed dye on the surface
photocatalytic parameter	bandgap	light absorption	UV/vis-DRS
	charge carrier kinetics	lifetime charge carriers	TRMC
	reactivity	number of generated ROS (OH*, O_2^{-}*)	catalytic testing under Ar and O_2 atmosphere

measured at 629 and 554 nm for Acid Blue 9 and rhodamine B, respectively. According to quasi first-order kinetics, $\ln(C_0/C_t)$ was plotted versus the time, and the slope of a linear regression represents the kinetic constant.

3. RESULTS AND DISCUSSION

3.1. Material Synthesis and Characterization. Changing the pulse times of the Pt precursor from 20 s to 5 min, we could achieve loadings of Pt ranging from 0.04 wt % to about 0.7 wt % at a reaction temperature of 100 °C. We were able to precisely control the loading, which increases with pulse time (Figure S1). Higher loadings (up to 3.13 wt % Pt) were achieved by applying up to four ALD cycles of Pt(Me_3)-(MeCp) and O_2 at pulse times of 5 min each. After annealing in a H_2 atmosphere, the Pt-containing clusters were converted from an initial Pt(II) oxidation state (Figure S2a) to their more active metallic Pt(0) state (Figure S2b),[29] which has been confirmed by XPS with peaks arising at 71.28 eV (Pt $5f_{7/2}$) and 74.28 eV (Pt $5f_{5/2}$) (Figure S3). TEM pictures confirmed the homogeneously distributed deposition of Pt clusters on the surface of TiO_2 with an average particle size of about 1.4 nm (Figure 1).

3.2. Photocatalytic Degradation of Acid Blue 9 and Rhodamine B. The photocatalytic activity was evaluated by decolorization of the two differently charged dyes, Acid Blue 9, which is solely negatively charged in natural conditions, and rhodamine B, a positively charged zwitter-ionic molecule (pK_a = 3.7).[30] Both demonstrated a drastic increase in the photocatalytic activity, measured in natural pH, for the loading of 0.34 wt % Pt as compared to P25 for both Acid Blue 9 and rhodamine B, followed by an activity drop to even lower values than the intrinsic value of P25 for higher Pt loadings (>1.8 wt % Pt) (Figures 2 and S4). The initial slight decrease in activity for very low loadings around 0.1 wt % Pt observed for both dyes is likely caused by the deposition process. Despite annealing in a hydrogen atmosphere to convert the Pt into its metallic state, residues from the organic ligands might still be present at the surface of TiO_2 and have a negative effect on the photocatalytic activity.[11] This is very apparent, especially for the very low loaded samples, where the contamination may overpower the positive effect of the Pt deposition.

Despite the well-established behavior of Pt on TiO_2 as a photocatalyst for dye degradation of showing an optimum,[31−33] it still gives rise to the question what is the mechanism behind this initial increase and especially the subsequent drop to a lower activity as compared to pure P25 for higher Pt loadings. It has been proposed in earlier studies that Pt on TiO_2 acts as an electron collector, making the lifetime of the separated electron and hole longer[13] allowing those to react with the pollutant or water to create radicals, enabling the degradation of the pollutants. This would explain the initial positive effect of the Pt but not why the activity drops to lower than P25 for higher Pt loadings. Logically there must be at least two mechanisms behind—at least one positive and one negative—which gives this optimal loading behavior, as discussed in the Introduction.

Because many parameters can affect the photocatalytic activity, Table 1 gives an indication of which factors might be influential to the overall photocatalytic activity.

In the following, we will elaborate on each material property individually in order to check in a systematic way the role of Pt on P25 as a photocatalyst:

3.2.1. Surface Area. For heterogeneous photocatalysis, the available surface area is an important parameter to describe the activity of a catalyst. Because the reaction takes place in dispersion, it should be described both by the overall surface,

https://dx.doi.org/10.1021/acs.jpcc.0c00926
J. Phys. Chem. C 2020, 124, 8269−8278

which is measured by BET analysis, and the available surface for the reaction where surface coverage of materials or agglomeration of catalyst particles can be a reducing factor. BET analysis yields a surface area of 54.75 m^2/g for Pt:P25 (0.34 wt % Pt), equal to P25 (from supplier, see Experimental Section), demonstrating that the deposited Pt clusters have only an insignificant effect on the BET surface area. However, because photocatalytic testing takes place in a dispersion of water, a change in the agglomerate size might influence the mass transfer of reactants to the inner surface of agglomerates and, therefore, the overall photocatalytic activity.[34] Dynamic light scattering (DLS) showed a slight increase in the agglomerate size (*z*-average diameter) from 312 ± 24 nm (P25) to 408 ± 64 nm upon deposition of Pt clusters (0.34 wt % Pt) (Figure 3a). The additional agglomeration is likely

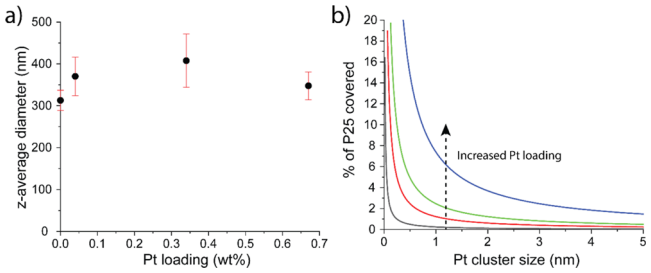

Figure 3. (a) *z*-average diameter from DLS measurements of P25 and differently loaded Pt:P25 catalysts. (b) Calculated coverage of Pt on the P25 surface as a function of the Pt cluster size for four different Pt loadings: 0.1 wt % (black), 0.5 wt % (red), 1 wt % (blue), and 3 wt % (green).

caused due to the deposition process where reactions of molecules on the surface might act as a "glue" between particles. However, the additional agglomeration is independent of the Pt loading and therefore acts more as a constant negative effect rather than as a dependency on the Pt loading. The reduced accessible surface due to stronger agglomeration might contribute to the small drop in activity for very low loadings up to 0.1 wt % Pt.[34] Furthermore, Pt, itself acting as a co-catalyst on the surface of P25, may reduce the active TiO_2 surface area for reactants. Taking into account the average Pt cluster size deposited on the TiO_2 surface of 1−2 nm, the surface coverage with Pt clusters only shows a limited decrease of less than 5% of the TiO_2 surface, with increasing Pt cluster size, especially for low loadings (Figure 3b). This indicates that the surface coverage of Pt on P25 also should not be an influential factor on the photocatalytic activity.

3.2.2. Reactant Adsorption. Dependent on the predominant reaction mechanism, the adsorption of the reactants plays an essential role in heterogeneous photocatalysis, that is, direct oxidation of the dye at the surface. The surface charge majorly influences the attraction or repulsion of differently charged molecules. The zeta potential often serves as an indication for the relative amount and the nature of charge present at the surface. Upon deposition of Pt, the zeta potential of the catalyst particles remains positive and at about +30 mV (Figure 4a) measured at a pH of 7.7 ± 0.3. Positive charges are present at the surface of both P25 and Pt:P25 due to the protonated −OH groups. Dye adsorption measurements (measured at a high powder concentration, see Experimental Section) of the negatively charged dye Acid Blue 9 and differently charged dye rhodamine B are in agreement with the positive zeta potential.

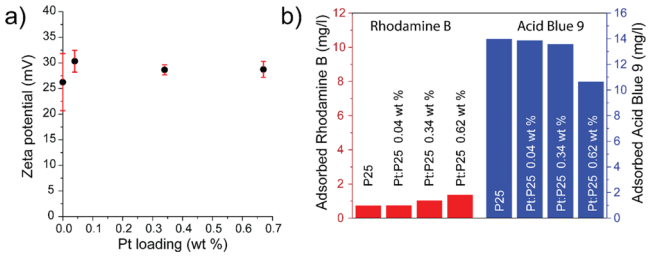

Figure 4. (a) Zeta-potential of various Pt-loaded TiO_2 (P25) samples. (b) Dye adsorption studies with a catalyst concentration of 2 g/L. Red bars indicate the amount of adsorbed rhodamine B on the surface of various loaded Pt:P25, and blue bars indicate the adsorption of Acid Blue 9 on the surface of Pt:P25. Samples were taken after 30 min of stirring in the dark.

As expected, Acid Blue 9 strongly adsorbs on the surface of both P25 and Pt:P25, whereas rhodamine B shows limited adsorption due to only weak interaction with the TiO_2 surface (Figure 4b). The Acid Blue 9 adsorption decreases for higher Pt loadings, while rhodamine B adsorbs accordingly slightly better to the surface, indicating that the zeta potential slightly decreases for higher Pt loadings. Despite the opposite adsorption behavior of rhodamine B and Acid Blue 9, the photocatalytic activity to degrade Acid Blue 9 and rhodamine B shows similar optimal behavior as a function of the Pt loading. This demonstrates that differences in dye adsorption have no impact on the general photocatalytic behavior of Pt:P25 versus pure P25.

Summarizing the external effects of surface area and pollutant adsorption of Pt:P25 compared to P25, we can conclude that both properties play if at all only a minor role on the dependence of the photocatalytic activity on Pt loading. Both the surface area measured by BET and the calculated actual free TiO_2 surface area from the surface coverage of Pt clusters only show a minor decrease. The agglomerate size instead generally increases for Pt:P25 which is due to the deposition process rather than related to the loading. Furthermore, the adsorption studies of different pollutants demonstrated the independence of the general photocatalytic behavior on the pollutant adsorption because for both cases of high and low reactant adsorption—dependent on the charge of the dye—Pt:P25 shows the same trend in photocatalytic activity as a function of the Pt loading.

After discussing the influence of the external parameters, we now will look more into the photo-catalytic parameters, that is, light absorption, charge carrier kinetics, and reactivity.

3.2.3. Light Absorption and Charge Carrier Dynamics. A common approach in photocatalyst development is to reduce the bandgap of the material in order to increase the photon absorption of the solar spectrum. This approach usually requires the incorporation of heteroatoms into the crystal lattice of the base material. In contrast, our deposition of Pt clusters on the TiO_2 surface is not expected to change the bandgap of TiO_2. However, Pt clusters may absorb light of all wavelengths as a result of the metallic character. The UV/vis-DRS spectra show increased absorption in the visible at higher Pt loadings (Figure 5a), which is caused by metallic Pt clusters.[12,35] Plasmonic effects for Pt-nanosized clusters are reported in the far UV range and can therefore not be a contributing factor to the increased visible light absorption of Pt:TiO_2(P25).[36] On the other hand, the presence of Pt clusters do not change the absorption edge, which indicates the

https://dx.doi.org/10.1021/acs.jpcc.0c00926
J. Phys. Chem. C 2020, 124, 8269−8278

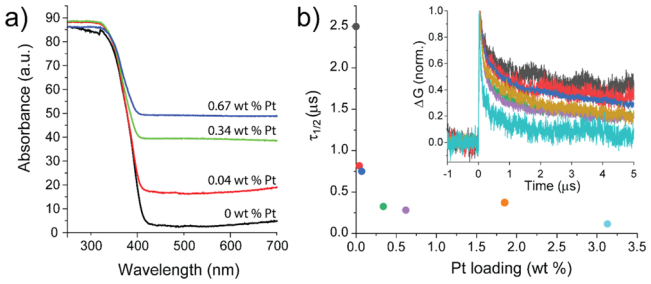

Figure 5. (a) Absorption spectrum UV/vis DRS spectra for different loaded Pt:P25. (b) Half time ($\tau_{1/2}$) of the mobile charge carriers measured by TRMC. Inset: transient decay of the mobile charge carrier.

bandgap of TiO_2 remains unaffected disregarding possible band bending near a junction to Pt. This is also expected because Pt(0) clusters are deposited on the surface and Pt is not incorporated in the TiO_2 lattice. Additionally, it indicates that possible other valencies (i.e. Pt(II) and Pt(IV)of Pt) were reduced to Pt(0) by H_2 post-treatment and are not affecting the band structure of TiO_2.

Light absorption by TiO_2 leads to the creation of mobile electrons and holes. The mobile electrons may transfer into the Pt clusters that allow redox reactions to occur. The electrons that transfer into the Pt clusters become immobile. With the microwave conductivity technique, the decrease in TiO_2 photoconductance is probed owing to the loss of free and mobile electrons in TiO_2 resulting from charge transfer to Pt. As the electrons in small noble metal clusters are immobile, no photoconductivity can come from these transferred electrons.[37] As such, the kinetics of the photoconductance transients provide a value for the charge transfer to Pt on the nanosecond to microsecond timescale. The half-life ($\tau_{1/2}$) of the free electrons in TiO_2 decreases with increasing Pt loadings (Figure 5b), which clearly indicates that the charge carrier dynamics are affected by the presence of Pt at the TiO_2 nanocrystal surface. Even at very low Pt loadings of 0.04 wt %, the effect is very pronounced. This shows that electron transfer from TiO_2 to Pt is energetically favorable and therefore supports charge separation. The transferred electrons in the Pt

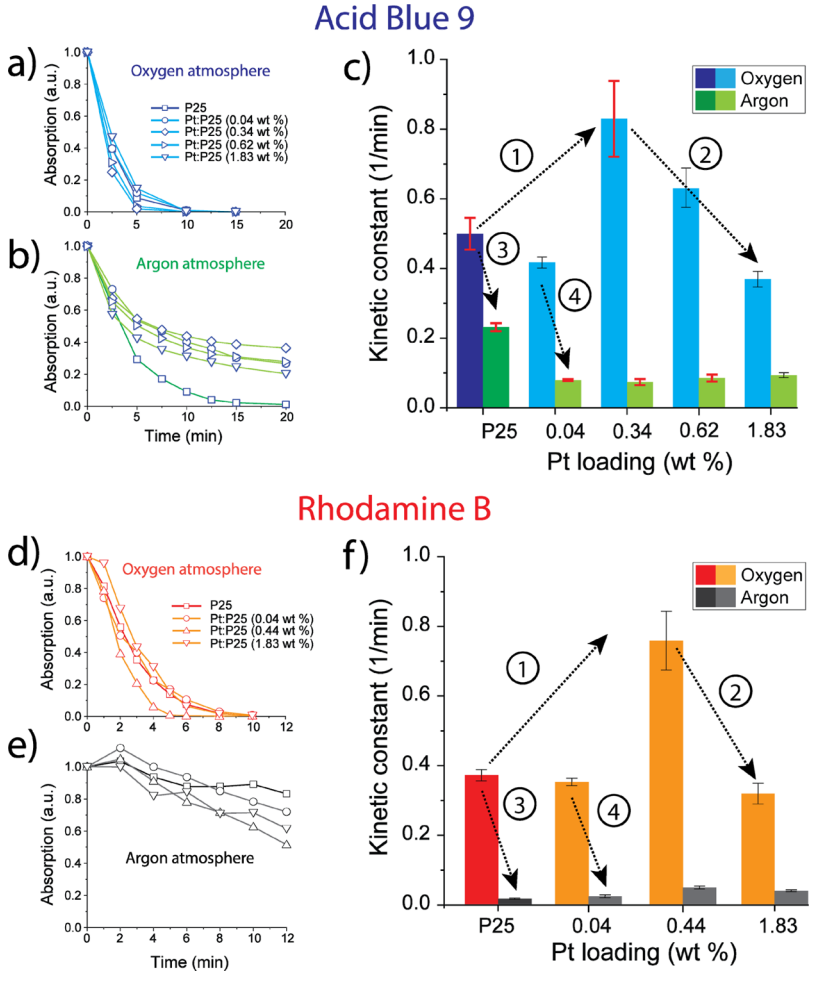

Figure 6. Degradation of different dyes in Ar and Oxygen atmosphere: (a) Time-dependent absorption of dissolved Acid Blue 9 in solutions of P25 with various Pt catalyst loadings in an O_2 atmosphere and (b) in an Ar atmosphere. (c) Kinetic constants for the conversion of Acid Blue 9 at different Pt catalyst loadings in an O_2 (blue, 0−5 min, more information see Supporting Information Figure S4) and Ar atmosphere (green, 10−20 min, more information see Supporting Information Figure S4). (d) Time-dependent absorption of dissolved rhodamine B in dispersions of P25 with various Pt catalyst loadings in an O_2 and (e) Ar atmosphere. (f) Kinetic constants for the conversion of rhodamine B at different Pt catalyst loadings under an O_2 atmosphere (red) and Ar atmosphere (black), red error bars represent the standard error of repeated experiments, and black error bars indicate the standard error form the linear regression fitting the kinetic constant.

https://dx.doi.org/10.1021/acs.jpcc.0c00926
J. Phys. Chem. C 2020, 124, 8269−8278

clusters may support different reactions determining the fate of the electrons. Pt is not only well known as an H_2 evolution catalyst by reducing H^+ with the collected electrons[38,39] but is also shown to readily adsorb O_2 on its surface.[18,20] The reduction of adsorbed O_2 to O_2^{-}* superoxide radical by the collected electrons would positively influence the photocatalytic activity for pollutant degradation improving the generation of ROS.[9] Therefore, photocatalytic degradation experiments using different environments, such as dispersions saturated with O_2 and Ar atmosphere, would give insight into the influence of adsorbed O_2 on the photocatalytic activity of Pt:P25. Excluding O_2 from the reaction medium will block the generation of superoxide O_2^{*-} radicals via the consumption of the CB electrons. The photocatalytic activities for various Pt loadings under saturated O_2 and Ar atmosphere are displayed in Figure 6.

Interestingly, we can observe four different effects (indicated by the numbers in Figure 6c,f:

(1) Under O_2 atmosphere, the photocatalytic activity increases to the maximum at 0.34 wt % Pt for both dyes (all tested Pt:P25 samples for rhodamine B and Acid Blue 9 degradation depicted in Figure 2).
(2) Further increase in the loading of Pt decreases the photocatalytic activity to even lower values than P25 for both dyes (see also Figure 2).
(3) Photoactivity only halves for P25 in an Ar atmosphere for Acid Blue 9 but significantly diminishes for the degradation of rhodamine B.
(4) For both dyes, the photocatalytic activity drops drastically in an Ar atmosphere for all Pt:P25 samples.

The degradation of rhodamine B in an inert atmosphere results in a strong suppression of the photocatalytic activity for both P25 and Pt:P25 (Figure 6f). For Acid Blue 9, the behavior is different. While the argon atmosphere hampers the activity of Pt:P25 drastically, especially in the later stage of the reaction, a significantly higher activity remains for P25 compared to Pt:P25 (Figure 6a−c). These results show that dissolved O_2 is a crucial factor in the degradation of both dyes. Without O_2 dissolved in the water, Pt:P25 is a worse catalyst than pure P25 for the degradation of Acid Blue 9. Because the electron transfer within materials is usually not influenced by conditions in the solution, the photogenerated electrons will transfer in both cases (O_2 and Ar atmosphere) to the Pt clusters raising the question about the fate of the electrons in the Pt clusters. Two options can be proposed: (1) the electrons are harvested from the surface of the Pt cluster to generate ROS and (2) in case no electron harvesting at the surface is possible, additional photo-generated electrons will charge up the Pt cluster, increasing the probability of charge recombination at the Pt−TiO_2 interface.

In an oxygen atmosphere, the dissolved O_2 will adsorb on the surface of Pt and subsequently consume the electrons available in the Pt cluster to generate superoxide (O_2^{-}*) radicals, which will degrade the dyes in the water. In the case of an Ar atmosphere, the electrons cannot react with O_2 and, therefore, will not be able to assist this photocatalytic degradation route. Nevertheless, this would still allow the holes in TiO_2 to react on the surface to generate OH radicals or degrade the dye directly. However, the activity drops drastically for Pt:P25, which demonstrates that not only neither of the degradation pathways (via direct oxidation, via hydroxyl or superoxide radical formation) but also other sacrificial reactions such as H_2 evolution (which could harvest the electrons from the Pt clusters and allow degradation pathway via the VB) are not very active under these conditions of an argon atmosphere. This behavior suggests to be caused by the intrinsic behavior of Pt. Theoretical calculations from Muhich et al.[18] indicate that Pt (in addition to an electron collector) also acts as an electron−hole recombination center, where electrons and holes recombine in the Pt cluster, and this affects the activity more predominantly when the electrons cannot be harvested by O_2, leading to a worse photocatalytic activity compared to TiO_2. On the other hand, according to Muhich's calculations, Pt clusters on the surface of TiO_2 will improve the adsorption of O_2 with respect to the intrinsic TiO_2 surface, improving the ROS formation to degrade organic pollutants faster.[18] From our results, it becomes clear that for low Pt loadings, O_2 can easily consume all the electrons from the few Pt clusters because the surface of Pt is supplied with enough O_2 so that the benefit of electron consumption by adsorbed O_2 is stronger than the recombination of electrons with holes. As soon there is too much Pt on the surface, insufficient O_2 can be provided for the consumption of all electrons provided by the Pt-surface due to diffusion limiting the transport of O_2 to the Pt-surface, which leads to a more pronounced electron−hole recombination at the Pt−TiO_2 interface becoming the rate-limiting step in the reaction mechanism. This interaction between a beneficial (O_2 adsorption and electron consumption) effect and a disadvantageous (electron−hole recombination) effect explains why an optimal Pt loading for the photocatalytic degradation of dyes by TiO_2−Pt is observed. In this context, it is expected that not only the Pt loading but also the Pt cluster size and morphology will play an essential role[40,41] in the O_2 adsorption versus charge recombination mechanism due to the difference in the surface to volume ratio, which would be a relevant property to investigate in future research.

The degradation of rhodamine B under an argon atmosphere is majorly obstructed for both P25 and Pt:P25 (Figure 6d−f). The difference to Acid Blue 9 is the charge and the related adsorption on the surface. The zwitterionic rhodamine B molecule does not adsorb on the surface due to only weak electrostatic interactions (Figure 4b). This means that a direct degradation of dyes via holes in the TiO_2 VB is unlikely. Similarly, dye degradation via surface-generated OH* has no substantial contribution. Without both, this degradation mechanism and the dominance of the consumption of the CB electrons by O_2, the photocatalytic activity drops to a minimum as a result of the charge recombination. In contrast, P25 readily degrades Acid Blue 9 in an Ar atmosphere. This is caused by the degradation reaction of free holes in TiO_2 with absorbed Acid Blue 9. However, the fate of excited electrons in the CB remains unclear from our present experiments. One possibility is that electrons may be harvested by either other sacrificial reactions such as reduction of water or the adsorbed dye molecules, but this investigation is beyond the scope of this study. This finding substantiates that direct oxidation has a high significance in the degradation pathway of Acid Blue 9 using P25.

In the case of Pt:P25 samples, the activity changes for Acid Blue 9 degradation in an Ar atmosphere throughout the experiment from an initial higher value (0−10 min), which is about 50% lower than that of P25, to a very low activity after 10 min (Figures S4 and S5). Despite that difference in activity according to first-order kinetics, applying those kinetics gives a

https://dx.doi.org/10.1021/acs.jpcc.0c00926
J. Phys. Chem. C 2020, 124, 8269−8278

chance to still compare both cases. The higher activity in the beginning (0−10 min), indicating a deviation from pure quasi first-order kinetics during the whole course of the reaction, could have two reasons. Because Acid Blue 9 adsorbs on the surface, the degradation on Pt:P25 occurs via the generated holes from TiO_2. The electrons will transfer to the Pt clusters, where the harvesting of electrons due to a lack of O_2 is not possible, which leads to a charge up of the Pt increasing the recombination rate with the holes in TiO_2. Second, Pt is often used as an oxygen reduction catalyst[40] and readily adsorbs oxygen at its surface. Even with extensive degassing via sonication while purging with Ar and a continuous Ar flow prior to the reaction, the Pt nanoclusters might be able due to strong interaction with O_2 to bind oxygen at its surface. This limited amount of oxygen, bound on the Pt surface, is consumed in the first stages of the irradiation to harvest the electrons in the Pt, leading to decomposition of the adsorbed Acid Blue 9 with a high reaction rate. After depletion of the remaining dissolved and adsorbed O_2, the kinetic constant further drops due to the increasing probability of charge recombination of the electrons in the Pt clusters with the holes in TiO_2. However, this behavior of an initial higher kinetic constant is not observed for the degradation of rhodamine B in an Ar atmosphere, drawing the importance toward the adsorption of the pollutant. Therefore, it is more likely that the direct oxidation due to adsorption of Acid Blue 9 is the determining factor for this behavior.

Summarizing the photocatalytic properties, Pt clusters on P25 nanoparticles do not affect the creation of charge carriers by light absorption in TiO_2, observing only an absorption increase in the range of visible light caused by the metallic state of Pt itself but no change in the UV-absorption properties of TiO_2. However, with higher loading, the Pt clusters themselves will absorb and consequently block light reaching the TiO_2 surface with a possible negative influence on the photocatalytic activity. The fate of charge carriers is strongly determined by the deposition of Pt clusters. Photogenerated electrons are separated from the holes by transferring to the Pt clusters and will react further in the presence of O_2 to generate reactive oxygen species. On the other hand, in case no O_2 is present, electrons will not be consumed by sacrificial redox reactions but easily recombine with the holes in TiO_2, inhibiting the photocatalytic activity (Figure 7). This makes the presence of

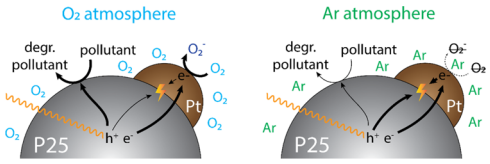

Figure 7. Proposed mechanism of photocatalytic dye decomposition for Pt:P25 in O_2 (left) and Ar (right) atmosphere, and the thickness of the arrows indicates the probability of the events.

sufficient O_2 the crucial factor determining the efficiency of the photocatalytic degradation of dyes using Pt:P25 because dissolved O_2 will harvest the separated electrons in the Pt cluster preventing the electron−hole recombination independent of the pollutant.

This study evaluated the photocatalytic activity at a natural pH. Avoiding the addition of acids/bases to adjust the pH avoids the contamination with additional ions which may also act as a scavenger influencing the generation of reactive oxygen species. Nevertheless, for further implantation into applications, the photocatalytic activity of Pt:P25 (TiO_2) also should be investigated at different pH values and should be subject to follow-up studies. Nevertheless, this detailed insight into the photocatalytic dye-degradation mechanism using Pt:P25 gives the opportunity to smartly design photocatalytic materials that optimize different parts of the photocatalysis mechanism, such as the improvement of light absorption or the efficient generation of ROS via electrons in the CB. Furthermore, understanding the behavior in different atmospheres is especially valuable for later developments of bringing the Pt:P25 photocatalyst into practice where contaminated water sources might suffer a lack of oxygen due to external influences such as algae growth.

4. CONCLUSIONS

Using an atomic layer deposition, we deposited Pt clusters on TiO_2 (P25) nanoparticles at a temperature as low as 100 °C. Depositing various loadings of Pt (0.04−3.13 wt % Pt) gave us the opportunity to investigate the role of Pt on TiO_2 (P25) for a range of Pt loadings on the photocatalytic degradation of Acid Blue 9 and rhodamine B. The synthesized Pt:P25 catalysts exhibited an optimal photocatalytic activity at very low loadings (i.e. 0.36 wt % Pt) for the degradation of Acid Blue 9 and rhodamine B under ambient conditions. However, experiments under Ar versus O_2 atmosphere demonstrated the importance of O_2 dissolved in the reactor suspension. Testing the degradation of two different pollutants under inert conditions (Ar atmosphere), the Pt:P25 catalyst showed a tremendous decrease in activity compared to the reaction under an O_2 atmosphere, independent of the Pt loading, whereas P25 remained partly active for the degradation of Acid Blue 9. It can be concluded that O_2 is the critical factor to efficiently harvest the electrons which are separated at the TiO_2−Pt interface and transferred to the Pt clusters. Without the consumption of electrons by O_2 at the Pt surface, the recombination of electrons in the Pt and holes at the Pt−TiO_2 interface dominates the reaction mechanism, leading to a poor photocatalytic activity. In an O_2 atmosphere, for low loadings of Pt, the consumption of electrons by oxygen adsorbed on the Pt surface plays the predominant role in enhancing the photocatalytic activity. At higher Pt loadings, the disadvantageous charge recombination properties of Pt exceed the positive effects of O_2 adsorption, and the overall photocatalytic efficiency drops even below the initial value of P25. These findings add experimental proof to the theoretically proposed reaction mechanism by Muhich et al.[18]

■ ASSOCIATED CONTENT

Supporting Information

The Supporting Information is available free of charge at https://pubs.acs.org/doi/10.1021/acs.jpcc.0c00926.

Material characterization and details on the degradation versus time for the degradation of the used dyes resulting in the calculation of the kinetic constants (PDF)

■ AUTHOR INFORMATION

Corresponding Authors

Dominik Benz − *Product & Process Engineering, Department of Chemical Engineering, Faculty of Applied Sciences, Delft University of Technology, 2629 HZ Delft, The Netherlands;*

https://dx.doi.org/10.1021/acs.jpcc.0c00926
J. Phys. Chem. C 2020, 124, 8269−8278

orcid.org/0000-0001-9025-0174; Email: d.benz@tudelft.nl

J. Ruud van Ommen − *Product & Process Engineering, Department of Chemical Engineering, Faculty of Applied Sciences, Delft University of Technology, 2629 HZ Delft, The Netherlands;* orcid.org/0000-0001-7884-0323; Email: J.R.vanOmmen@tudelft.nl

Authors

Kevin M. Felter − *Optoelectronic Materials Section, Department of Chemical Engineering, Faculty of Applied Sciences, Delft University of Technology, 2629 HZ Delft, The Netherlands;* orcid.org/0000-0002-5316-6405

Jan Köser − *Chemical Process Engineering, Faculty of Production Engineering, University of Bremen, 28359 Bremen, Germany*

Jorg Thöming − *Chemical Process Engineering, Faculty of Production Engineering, University of Bremen, 28359 Bremen, Germany;* orcid.org/0000-0002-5374-114X

Guido Mul − *Photocatalytic Synthesis Group, Faculty of Science and Technology, University of Twente, 7500 AE Enschede, The Netherlands;* orcid.org/0000-0001-5898-6384

Ferdinand C. Grozema − *Optoelectronic Materials Section, Department of Chemical Engineering, Faculty of Applied Sciences, Delft University of Technology, 2629 HZ Delft, The Netherlands;* orcid.org/0000-0002-4375-799X

Hubertus T. Hintzen − *Group Luminescent Materials, Section Fundamental Aspects of Materials and Energy, Faculty of Applied Sciences, Delft University of Technology, 2629 HZ Delft, The Netherlands*

Michiel T. Kreutzer − *Product & Process Engineering, Department of Chemical Engineering, Faculty of Applied Sciences, Delft University of Technology, 2629 HZ Delft, The Netherlands*

Complete contact information is available at: https://pubs.acs.org/10.1021/acs.jpcc.0c00926

Notes

The authors declare no competing financial interest.

■ ACKNOWLEDGMENTS

We would like to thank Bart van der Linden from the Catalysis Engineering group at TU Delft for support in photocatalytic experiments under different atmospheres as well as Willy Rook for executing the BET analysis form the same group. Furthermore, we would like to acknowledge Ruben Abellon for his help in the UV/vis-DRS measurements. This research is supported by the TU Delft | Global Initiative, a program of the Delft University of Technology to boost Science and Technology for Global Development.

■ REFERENCES

(1) Zhang, J.; Nosaka, Y. Mechanism of the OH Radical Generation in Photocatalysis with TiO_2 of Different Crystalline Types. *J. Phys. Chem. C* **2014**, *118*, 10824−10832.

(2) Linsebigler, A. L.; Lu, G.; Yates, J. T. Photocatalysis on TiO_2 Surfaces: Principles, Mechanisms, and Selected Results. *Chem. Rev.* **1995**, *95*, 735−758.

(3) Mortazavian, S.; Saber, A.; James, D. E. Optimization of Photocatalytic Degradation of Acid Blue 113 and Acid Red 88 Textile Dyes in a Uv-C/TiO_2 Suspension System: Application of Response Surface Methodology (Rsm). *Catalysts* **2019**, *9*, 360.

(4) Ahmed, S.; Rasul, M. G.; Martens, W. N.; Brown, R.; Hashib, M. A. Heterogeneous photocatalytic degradation of phenols in wastewater: A review on current status and developments. *Desalination* **2010**, *261*, 3−18.

(5) Reza, K. M.; Kurny, A.; Gulshan, F. Parameters Affecting the Photocatalytic Degradation of Dyes Using TiO_2: A Review. *Appl. Water Sci.* **2015**, *7*, 1569−1578.

(6) Motegh, M.; van Ommen, J. R.; Appel, P. W.; Kreutzer, M. T. Scale-up Study of a Multiphase Photocatalytic Reactor-Degradation of Cyanide in Water over TiO_2. *Environ. Sci. Technol.* **2014**, *48*, 1574−1581.

(7) Gaya, U. I. Mechanistic Principles of Photocatalytic Reaction. In *Heterogeneous Photocatalysis Using Inorganic Semiconductor Solids*; Gaya, U. I., Ed.; Springer Netherlands: Dordrecht, 2014; pp 73−89.

(8) Hoffmann, M. R.; Martin, S. T.; Choi, W.; Bahnemann, D. W. Environmental Applications of Semiconductor Photocatalysis. *Chem. Rev.* **1995**, *95*, 69−96.

(9) Gaya, U. I. Principles of Heterogeneous Photocatalysis. *Heterogeneous Photocatalysis Using Inorganic Semiconductor Solids*; Springer Netherlands: Dordrecht, 2014; pp 1−41.

(10) Goulas, A.; Ruud van Ommen, J. Atomic Layer Deposition of Platinum Clusters on Titania Nanoparticles at Atmospheric Pressure. *J. Mater. Chem. A* **2013**, *1*, 4647−4650.

(11) Zhou, Y.; King, D. M.; Liang, X.; Li, J.; Weimer, A. W. Optimal Preparation of Pt/TiO_2 Photocatalysts Using Atomic Layer Deposition. *Appl. Catal., B* **2010**, *101*, 54−60.

(12) Driessen, M. D.; Grassian, V. H. Photooxidation of Trichloroethylene on Pt/TiO_2. *J. Phys. Chem. C* **1998**, *102*, 1418−1423.

(13) Nasr, O.; Mohamed, O.; Al-Shirbini, A.-S.; Abdel-Wahab, A.-M. Photocatalytic Degradation of Acetaminophen over Ag, Au and Pt Loaded TiO_2 Using Solar Light. *J. Photochem. Photobiol., A* **2019**, *374*, 185−193.

(14) Vaiano, V.; Iervolino, G.; Sannino, D.; Murcia, J. J.; Hidalgo, M. C.; Ciambelli, P.; Navío, J. A. Photocatalytic Removal of Patent Blue V Dye on Au-TiO_2 and Pt-TiO_2 Catalysts. *Appl. Catal., B* **2016**, *188*, 134−146.

(15) Ofiarska, A.; Pieczyńska, A.; Fiszka Borzyszkowska, A.; Stepnowski, P.; Siedlecka, E. M. Pt−TiO_2-Assisted Photocatalytic Degradation of the Cytostatic Drugs Ifosfamide and Cyclophosphamide under Artificial Sunlight. *Chem. Eng. J.* **2016**, *285*, 417−427.

(16) Kryukova, G.; Zenkovets, G.; Shutilov, A.; Wilde, M.; Gunther, K.; Fassler, D.; Richter, K. Structural Peculiarities of TiO_2 and Pt/TiO_2 Catalysts for the Photocatalytic Oxidation of Aqueous Solution of Acid Orange 7 Dye Upon Ultraviolet Light. *Appl. Catal., B* **2007**, *71*, 169−176.

(17) Angeline Dorothy, A.; Subramaniam, N. G.; Panigrahi, P. Tuning Electronic and Optical Properties of TiO_2 with Pt/Ag Doping to a Prospective Photocatalyst: A First Principles Dft Study. *Mater. Res. Express* **2019**, *6*, 045913.

(18) Muhich, C. L.; Zhou, Y.; Holder, A. M.; Weimer, A. W.; Musgrave, C. B. Effect of Surface Deposited Pt on the Photoactivity of TiO_2. *J. Phys. Chem. C* **2012**, *116*, 10138−10149.

(19) Saputera, W. H.; Scott, J. A.; Friedmann, D.; Amal, R. Revealing the Key Oxidative Species Generated by Pt-Loaded Metal Oxides under Dark and Light Conditions. *Appl. Catal., B* **2018**, *223*, 216−227.

(20) Saputera, W. H.; Scott, J.; Ganda, N.; Low, G. K.-C.; Amal, R. The Role of Adsorbed Oxygen in Formic Acid Oxidation by Pt/TiO_2 Facilitated by Light Pre-Treatment. *Catal. Sci. Technol.* **2016**, *6*, 6679−6687.

(21) Pepin, P. A.; Lee, J. D.; Foucher, A. C.; Murray, C. B.; Stach, E. A.; Vohs, J. M. The Influence of Surface Platinum Deposits on the Photocatalytic Activity of Anatase TiO_2 Nanocrystals. *J. Phys. Chem. C* **2019**, *123*, 10477−10486.

(22) Hu, X.; Ji, H.; Wu, L. Singlet Oxygen Photogeneration and 2,4,6-Tcp Photodegradation at Pt/TiO_2 under Visible Light Illumination. *RSC Adv.* **2012**, *2*, 12378−12383.

(23) Vijayan, B. K.; Dimitrijevic, N. M.; Wu, J.; Gray, K. A. The Effects of Pt Doping on the Structure and Visible Light Photoactivity of Titania Nanotubes. *J. Phys. Chem. C* **2010**, *114*, 21262−21269.

(24) Bamwenda, G. R.; Tsubota, S.; Nakamura, T.; Haruta, M. Photoassisted Hydrogen Production from a Water-Ethanol Solution: A Comparison of Activities of Au:TiO_2 and Pt:TiO_2. *J. Photochem. Photobiol., A* **1995**, *89*, 177−189.
(25) Ding, X.; An, T.; Li, G.; Zhang, S.; Chen, J.; Yuan, J.; Zhao, H.; Chen, H.; Sheng, G.; Fu, J. Preparation and Characterization of Hydrophobic TiO_2 Pillared Clay: The Effect of Acid Hydrolysis Catalyst and Doped Pt Amount on Photocatalytic Activity. *J. Colloid Interface Sci.* **2008**, *320*, 501−507.
(26) van Ommen, J. R.; Goulas, A. Atomic Layer Deposition on Particulate Materials. *Mater. Today Chem.* **2019**, *14*, 100183.
(27) Beetstra, R.; Lafont, U.; Nijenhuis, J.; Kelder, E. M.; van Ommen, J. R. Atmospheric Pressure Process for Coating Particles Using Atomic Layer Deposition. *Chem. Vap. Deposition* **2009**, *15*, 227−233.
(28) Kroeze, J. E.; Savenije, T. J.; Warman, J. M. Electrodeless Determination of the Trap Density, Decay Kinetics, and Charge Separation Efficiency of Dye-Sensitized Nanocrystalline TiO_2. *J. Am. Chem. Soc.* **2004**, *126*, 7608−7618.
(29) Lee, J.; Choi, W. Photocatalytic Reactivity of Surface Platinized TiO_2: Substrate Specificity and the Effect of Pt Oxidation State. *J. Phys. Chem. B* **2005**, *109*, 7399−7406.
(30) Wang, P.; Cheng, M.; Zhang, Z. On Different Photo-decomposition Behaviors of Rhodamine B on Laponite and Montmorillonite Clay under Visible Light Irradiation. *J. Saudi Chem. Soc.* **2014**, *18*, 308−316.
(31) Alamelu, K.; Jaffar Ali, B. M. Tio2-Pt Composite Photocatalyst for Photodegradation and Chemical Reduction of Recalcitrant Organic Pollutants. *J. Environ. Chem. Eng.* **2018**, *6*, 5720−5731.
(32) Zhou, Y.; King, D. M.; Liang, X.; Li, J.; Weimer, A. W. Optimal Preparation of Pt/TiO_2 Photocatalysts Using Atomic Layer Deposition. *Appl. Catal., B* **2010**, *101*, 54−60.
(33) Siuzdak, K.; Sawczak, M.; Klein, M.; Nowaczyk, G.; Jurga, S.; Cenian, A. Preparation of Platinum Modified Titanium Dioxide Nanoparticles with the Use of Laser Ablation in Water. *Phys. Chem. Chem. Phys.* **2014**, *16*, 15199−15206.
(34) Mehrotra, K.; Yablonsky, G. S.; Ray, A. K. Kinetic Studies of Photocatalytic Degradation in a TiO_2 Slurry System: Distinguishing Working Regimes and Determining Rate Dependences. *Ind. Eng. Chem. Res.* **2003**, *42*, 2273−2281.
(35) Bumajdad, A.; Madkour, M. Understanding the Superior Photocatalytic Activity of Noble Metals Modified Titania under Uv and Visible Light Irradiation. *Phys. Chem. Chem. Phys.* **2014**, *16*, 7146−7158.
(36) Tajerian, T.; Monsefi, M.; Rowan, A. Simple Chemistry Drives Controlled Synthesis of Platinum Nanocrystal to Micron Size. *J. Nanostruct. Chem.* **2019**, *9*, 197−202.
(37) Carneiro, J. T.; Savenije, T. J.; Moulijn, J. A.; Mul, G. The Effect of Au on TiO_2 Catalyzed Selective Photocatalytic Oxidation of Cyclohexane. *J. Photochem. Photobiol., A* **2011**, *217*, 326−332.
(38) Kmetykó, Á.; Mogyorósi, K.; Gerse, V.; Kónya, Z.; Pusztai, P.; Dombi, A.; Hernádi, K. Photocatalytic H_2 Production Using Pt-TiO_2 in the Presence of Oxalic Acid: Influence of the Noble Metal Size and the Carrier Gas Flow Rate. *Materials* **2014**, *7*, 7022−7038.
(39) Dessal, C.; Martínez, L.; Maheu, C.; Len, T.; Morfin, F.; Rousset, J. L.; Puzenat, E.; Afanasiev, P.; Aouine, M.; Soler, L.; et al. Influence of Pt Particle Size and Reaction Phase on the Photocatalytic Performances of Ultradispersed Pt/TiO_2 Catalysts for Hydrogen Evolution. *J. Catal.* **2019**, *375*, 155−163.
(40) Xu, S.; Kim, Y.; Park, J.; Higgins, D.; Shen, S.-J.; Schindler, P.; Thian, D.; Provine, J.; Torgersen, J.; Graf, T.; et al. Extending the Limits of Pt/C Catalysts with Passivation-Gas-Incorporated Atomic Layer Deposition. *Nat. Catal.* **2018**, *1*, 624−630.
(41) Wang, D.; Liu, Z.-P.; Yang, W.-M. Revealing the Size Effect of Platinum Cocatalyst for Photocatalytic Hydrogen Evolution on TiO_2 Support: A Dft Study. *ACS Catal.* **2018**, *8*, 7270−7278.

https://dx.doi.org/10.1021/acs.jpcc.0c00926
J. Phys. Chem. C 2020, 124, 8269−8278